Multiphoton Excitation Fluorescence Microscopy and Spectroscopy of In Vivo Human Skin

Barry R. Masters,* Peter T. C. So,# and Enrico Gratton#
*Department of Anatomy and Cell Biology, Uniformed Services University of the Health Sciences, Bethesda, Maryland 20814, and #Laboratory of Fluorescence Dynamics, Department of Physics, University of Illinois at Urbana, Illinois 61801 USA

ABSTRACT Multiphoton excitation microscopy at 730 nm and 960 nm was used to image in vivo human skin autofluorescence from the surface to a depth of ~200 μm. The emission spectra and fluorescence lifetime images were obtained at selected locations near the surface (0–50 μm) and at deeper depths (100–150 μm) for both excitation wavelengths. Cell borders and cell nuclei were the prominent structures observed. The spectroscopic data suggest that reduced pyridine nucleotides, NAD(P)H, are the primary source of the skin autofluorescence at 730 nm excitation. With 960 nm excitation, a two-photon fluorescence emission at 520 nm indicates the presence of a variable, position-dependent intensity component of flavoprotein. A second fluorescence emission component, which starts at 425 nm, is observed with 960-nm excitation. Such fluorescence emission at wavelengths less than half the excitation wavelength suggests an excitation process involving three or more photons. This conjecture is further confirmed by the observation of the super-quadratic dependence of the fluorescence intensity on the excitation power. Further work is required to spectroscopically identify these emitting species. This study demonstrates the use of multiphoton excitation microscopy for functional imaging of the metabolic states of in vivo human skin cells.

INTRODUCTION

Two-photon excitation microscopy

The use of scanning optical microscopy to image biological systems at the cellular level has been aided by the development of various types of confocal microscopes. The main advantage of confocal microscopes, which use a spatial filter in front of the photodetector, is their increased axial resolution, which permits optical sectioning of thick tissues and cells and their subsequent computerized three-dimensional reconstruction (Wilson, 1984). An alternative technique is two-photon excitation microscopy (Denk et al., 1990), which uses a high-power near-infrared laser to focus the light into a diffraction-limited spot in which two-photon excitation of the chromophores occurs. The quadratic dependence of the excitation probability results in optical sectioning without the use of a spatial filter.

Two-photon imaging is particularly suitable for studying deep tissue. The near-infrared light used in the two-photon microscope can penetrate deeper in highly scattering tissues such as in vivo human skin than confocal microscopes operated with ultraviolet excitation. In addition, the two-photon light collection efficiency is higher than that obtainable with a standard point scanning confocal microscope, because two-photon excitation microscopy uses neither a pinhole nor descanning optics. The optical sectioning originates in the nonlinear absorption process. Therefore a large area detector can be used to maximize the collection efficiency of the fluorescence photons, which may be scattered as they travel through the turbid sample. In terms of tissue photodamage, the near-infrared radiation used in two-photon excitation is less phototoxic than ultraviolet radiation. The localization of the two-photon excitation volume to the focal plane further minimizes the volume in which tissue damage may occur.

Two-photon excitation laser scanning microscopy with excitation at 705 nm has been successfully applied to the three-dimensional functional imaging of the in situ cornea, based on the fluorescence of the naturally occurring reduced pyridine nucleotides, NAD(P)H (Piston et al., 1995). No emission spectra or lifetimes were measured in these studies. The cornea is almost transparent at this wavelength, and images based on NAD(P)H fluorescence were obtained to a depth of 400 μm, which is the central thickness of the rabbit cornea.

Three-photon excitation spectroscopy and microscopy

The feasibility of three-photon spectrosocopy has been demonstrated in the recent literature (Gryczynski et al., 1995, 1996; Szmacinski et al., 1996). Three-photon excitation is characterized by an excitation wavelength that is about three times the wavelength of the absorption, and the emitted intensity depends on the cube of the excitation light intensity. The feasibility of applying this technique to high-resolution microscopy has been demonstrated (Wokosin et al., 1995; Xu et al., 1996a,b). The three-photon image point spread function is expected to be superior to the two-photon excitation method (Gu, 1996).

Received for publication 14 November 1996 and in final form 24 February 1997.

Address reprint requests to Dr. Peter T. C. So, Room 3-461a, Department of Mechanical Engineering, Massachusetts Institute of Technology, 77 Massachusetts Ave., Cambridge, MA 02139. Tel.: 617-253-6552; Fax: 617-258-9346; E-mail: ptso@mit.edu.

0006-3495/97/06/2405/08 $2.00

Gryczynski and co-workers found that *N*-acetyl-L-tryptophanamide (NATA) could be excited at 840 nm using a mode-locked Ti:sapphire laser (Gryczynski et al., 1996). The emission spectra of NATA were the same for one-photon excitation at 280 nm as for infrared excitation. The emission intensity of NATA was found to depend on the cube of the laser power at 840 nm, consistent with simultaneous absorption of three photons. These results suggest that the intrinsic fluorescence of proteins may be excited using the fundamental output of a Ti:sapphire laser. Similar results are also obtained for 2,5-diphenyloxazole (PPO) with excitation at 870 nm (Gryczynski et al., 1995). Gryczynski et al. have also demonstrated that two- and three-photon processes can be obtained from the same chromophore as a function of excitation wavelength. They showed that the calcium fluorophore Indo-1 can be excited by simultaneous absorption of three photons at 885 nm (Gryczynski et al., 1995; Szmacinski et al., 1996), but the excitation of Indo-1 becomes a two-photon process when the wavelength is decreased to 820 nm.

Skin anatomy

The skin is divided into three layers: the epidermis, the dermis, and the subcutaneous tissue. The epidermis is the outermost portion of the skin and is composed of stratified squamous epithelium. The epidermal thickness varies from 50 μm on the eyelids to 1.5 mm on the palms and soles. Fig. 1 shows a drawing of a vertical section of human skin illustrating the different cellular layers.

The innermost layer of the epidermis consists of a single layer of cuboidal cells called basal cells. These cells differentiate and migrate toward the skin surface. The outer layer of the epidermis is called the stratum corneum, which is composed of flattened and dead cells. The basal cells of the epidermis divide, differentiate, and finally slough. As they migrate to the skin surface, the cells become more stratified and finally form the cornified layer of the stratum corneum. The stratum corneum is 10–20 μm thick, except on the soles of the feet and the palms, where it can be 500–600 μm thick.

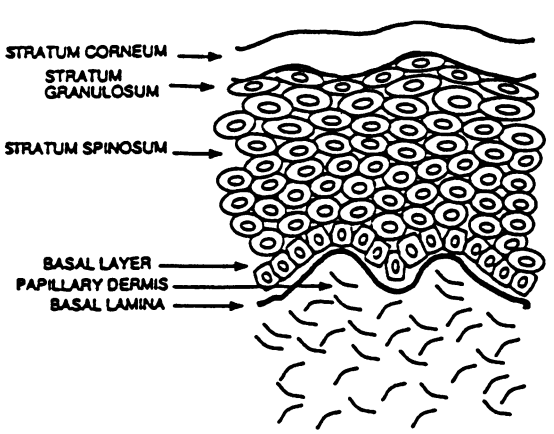

FIGURE 1 A drawing of the structure of a vertical section of human skin illustrating the cellular layers. The stratum corneum is located at the outer surface of the skin. The basal layer is the proliferative cell layer, which is the source of new cells in the skin. The epidermal layer corresponds to the skin structures above and including the layer of basal cells, and the skin structures below correspond to the dermal layer.

Confocal microscopy of skin

Several types of confocal microscopes have been developed using different designs for forming a two-dimensional image of a thin optical section within a thick specimen. The details of these scanning systems have been reviewed (Wilson, 1990; Pawley, 1995; Masters, 1995). A tandem scanning confocal microscope was developed by Petran and co-workers to optically section thick, highly scattering tissues in real time (Petran et al., 1968). This microscope has been adapted for the in vivo examination of skin by several researchers. In particular, Corcuff and co-workers have developed a real-time confocal microscope for in vivo skin imaging (Pierard et al., 1991; Corcuff and Leveque, 1993; Corcuff et al., 1993; Bertrand and Corcuff, 1994). These microscopes use an incoherent white light source and image the skin in the reflected light mode. The ability to visualize the full three-dimensional volume of in vivo human skin, based on a stack of optical sections, may have important diagnostic potential (Masters et al., 1996a).

A scanning laser confocal microscope for in vivo use has also been developed with video-rate imaging capabilities (Rajadhyaksha et al., 1995). This instrument, which operates with reflected light at laser wavelengths of 488 nm, 514 nm, 647 nm, and 800 nm, has been used for imaging human skin in vivo.

Skin autofluorescence

Skin autofluorescence originates from endogenous chromophores in tissues such as reduced pyridine nucleotides and flavoproteins. Autofluorescence of in vivo human skin with excitation at 488 nm and emission detected at wavelengths longer than 515 nm was studied with a laser scanning confocal microscope (Masters, 1996). Optical sections of the stratum corneum were obtained from the anterior surface of the index finger and the lower surface of the human forearm. Pseudocolor depth-coded projections were formed from stacks of optical sections. Individual cells could only be observed at the top surface of the skin. With ultraviolet excitation at 365 nm, the penetration depth was limited to the 20 μm of the stratum corneum at the skin surface. Although these studies were limited in the penetration achieved, the use of autofluorescence as a source of natural contrast for confocal microscopy of in vivo human skin was demonstrated. In the present study three-dimensional autofluorescence imaging of in vivo human skin was investigated with two- and three-photon excitation microscopy (730 nm and 960 nm). The fluorescence emission was

characterized with fluorescence spectroscopy and lifetime imaging techniques.

MATERIALS AND METHODS

Biological sample

The lower surface of the right forearm (of one of the authors) was placed on the microscope stage, where an aluminum plate with a 1-cm square hole was mounted. The square hole was covered by a standard cover glass. The skin was in contact with the cover glass to maintain a mechanically stable surface. The upper portion of the arm rested on a stable platform, which prevented motion of the arm during the measurements. The measurement time was always less than 10 min. The estimated power incident on the skin was 10–15 mW. The photon flux incident upon a diffraction-limited spot on the skin is on the order of 10 MW/cm^2.

Multiphoton scanning microscope

The schematic of the multiphoton scanning microscope is presented in Fig. 2. This two-photon scanning microscope has previously been described (So et al., 1995, 1996). A femtosecond Ti-sapphire laser (Mira 900; Coherent, Palo Alto, CA) tuned to either 730 nm or 960 nm was used as our light source. The power entering the microscope was adjusted to 100 mW via a Glan-Thompson polarizer. The microscope has a power transmission efficiency of 10–20%, resulting in 10–15 mW power incident upon the skin. The scanning is achieved via a galvanometer-driven x-y scanner (Cambridge Technology, Watertown, MA). The scan parameters are chosen such that 256 × 256 pixel images are generated with a pixel residence time of 40 μs corresponding to a frame rate of about 3 s. The excitation light enters the Zeiss Axiovert 35 microscope (Zeiss, Thornwood, NY) via a modified epiluminescence light path. The light is reflected by the dichroic mirror to the objective. Two objectives were used in these experiments: a Zeiss 40× Plan-Fluor (1.3 N.A., oil) is used for high-resolution imaging, and a Zeiss 20× Plan-Neofluor (0.75 N.A., air) is used for its longer working distance into the tissue. The lateral resolution of these objectives is calibrated using fluorescent latex spheres of known size. The 40× objective has a lateral resolution of 0.20 μm per pixel, corresponding to an image size of 51.2 μm. The 20× objective has a lateral resolution of 0.54 μm per pixel, corresponding to an image size of 137 μm. The fluorescence signal is collected by the same objective, transmitted through the dichroic mirror and barrier filter (3 mm BG-39; CVI Laser, CA), and refocused on the detector. The fluorescence signal at each pixel is detected by a photomultiplier tube (PMT). For intensity measurements, a low-noise, single photon counting R5600-P PMT or a high gain cooled R1104 PMT (Hamamatsu, Bridgewater, NJ) is used for single photon counting. The output of the PMT is converted to single photoelectron pulses via a low-noise amplifier/discriminator (Pacific AD6, Concord, CA). The number of photons collected at each pixel is counted and digitally recorded by the control computer (Intel 486; Gateway). Custom software synchronizes this data acquisition process with the scanner movement to generate a 2-D image. A 3-D imaged stack can be obtained by controlling the microscope objective height with a stepper motor; the microscope objective position is monitored using a linear variable differential transformer (Schaevitz Engineering, Camden, NJ). An image stack with a depth of up to 200 μm into the skin has been obtained. The typical depth increment used in these experiments was 5 μm. The image stack was stored digitally. Three-dimensional reconstruction and presentation were performed using Spyglass Slicer Software (Fortner Research, Sterling, VA).

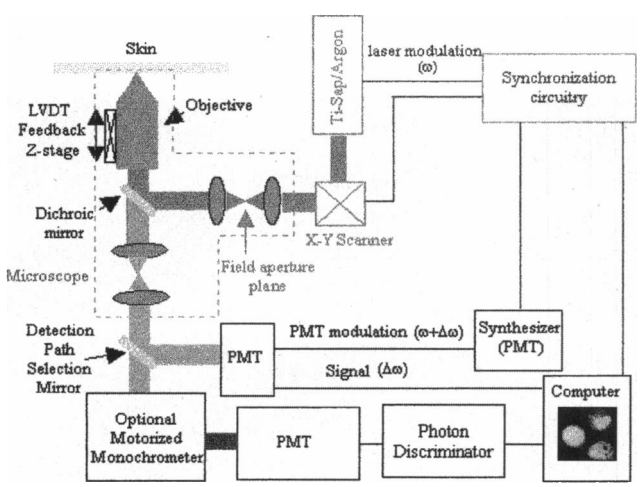

FIGURE 2 Schematic of the two-photon scanning microscope. Two detection beam paths are featured: one for measuring fluorescence lifetimes and the other for measuring emission intensity/spectrum. These two beam paths can be selected by rotating a single mirror. The PMT denotes the photomultiplier tube. The LVDT denotes a linear variable differential transformer. The Ti-sapphire/argon denotes the argon-ion laser pumped titanium-sapphire laser.

Measurement of the fluorescence emission spectrum in the microscope

We have performed measurements of the skin emission spectrum at selected points. A motor-driven monochromator is inserted between the microscope and the photomultiplier tube. The monochromator is driven at a constant speed of 1 nm/s. The wavelength resolution is set by the monochromator slit to 2 nm. The x-y scanner is set to remain at the origin during spectral measurement. Data were collected in photon counting mode. The fluorescence spectrum is measured at two excitation wavelengths of 730 and 960 nm. Spectra were taken at two depths: the surface (0–50 μm) and below the epidermis (100–150 μm).

Measurement of the fluorescence lifetime in the microscope

We have obtained fluorescence lifetime images of skin tissue using frequency-domain heterodyning techniques, which were previously described (So et al., 1995). A R3896 PMT (Hamamatsu, Bridgewater, NJ) that can be gain modulated by a synchronized synthesizer is used for these measurements (Alcala et al., 1985). Fluorescence lifetimes were measured with frequency-domain heterodyning at high cross-correlation frequencies. Lifetime images were collected at 730 nm and 960 nm. Lifetime images were also taken at two depths: at the surface (0–50 μm) and below the epidermis (100–150 μm). A modulation frequency of 80 MHz was used for these measurements. The pixel residence time had been increased to 640 μs to improve the signal-to-noise ratio. Three images were averaged and stored. Fluorescein in pH 8 buffer solution was used as the lifetime reference standard (4 ns). Pixels of the images were averaged for lifetime calculations, and single exponential decay was assumed for fluorescein.

Measurement of the fluorescence intensity dependence on excitation power

We have measured the fluorescence intensity as a function of excitation power to determine whether the excitation at 960 nm is due to two-photon excitation or involves higher photon processes. A 0.5-mm-thick slice of human skin from the second digit of the right hand was excised. The sample was sandwiched between a piece of cover glass and a microscope slide. The fresh sample was imaged immediately. The incident power was controlled by a polarizer. Fluorescence images of the same area were collected at power levels ranging from 1 to 10 mW with 960 nm excitation.

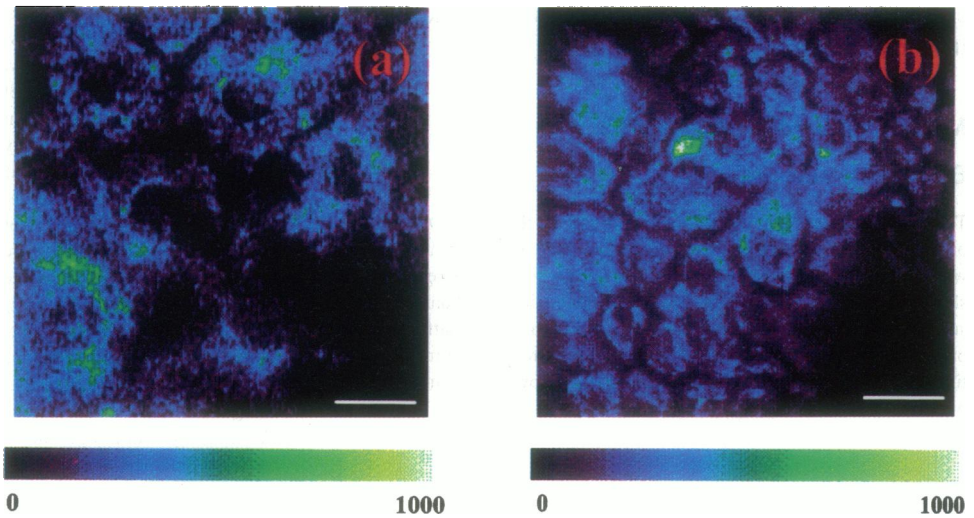

FIGURE 3 Representative multiphoton images of two cell layers with an excitation wavelength of 730 nm. (*a*) A cell layer at a depth between 40 and 60 μm from the skin surface. (*b*) A cell layer at a depth between 30 and 50 μm from the skin surface. The scale bar corresponds to 10 μm.

Equivalent portions (10 × 10 pixel areas) of these images were averaged and compared.

RESULTS AND DISCUSSION

Multiphoton imaging of in vivo human skin

We observed individual cells within the thickness of the skin at depths from 25 to 75 μm below the skin surface (Fig. 3). No cells were observed within the stratum corneum. This is consistent with studies using reflected light confocal microscopy. At lower depths, fluorescent images of the cellular cytoplasm were observed. This is consistent with the assumption that NAD(P)H provides the major contribution to the cellular autofluorescence observed. The cell nuclei and the cell borders appear dark because of the absence of fluorescence. Cells of 15–20 μm diameter were imaged at an approximate depth of 40–50 μm. Cells of ~8–10 μm diameter were observed at an average depth of 25–30 μm. This is consistent with reflected light confocal microscope results indicating a decrease in cell size at the shallower depths. Within the cytoplasm of the larger cells, punctuated fluorescence can be observed. This is consistent with previous isolated single cell studies (Koenig et al., 1996), and these fluorescent organelles are likely to be mitochondria with a high concentration of NAD(P)H.

Image stacks of human skin were obtained at both 730 nm and 960 nm excitation. A representative montage of images from a complete stack is shown in Fig. 4. Excitation power of about 10 mW was used throughout these experiments. The fluorescence signal decreased for deeper images, as expected from the exponential decrease of light transmission in a highly scattering medium. In Fig. 4 *b*, the semicircular dark region may correspond to a sweat duct about 20 μm below the surface of the skin. Individual cells

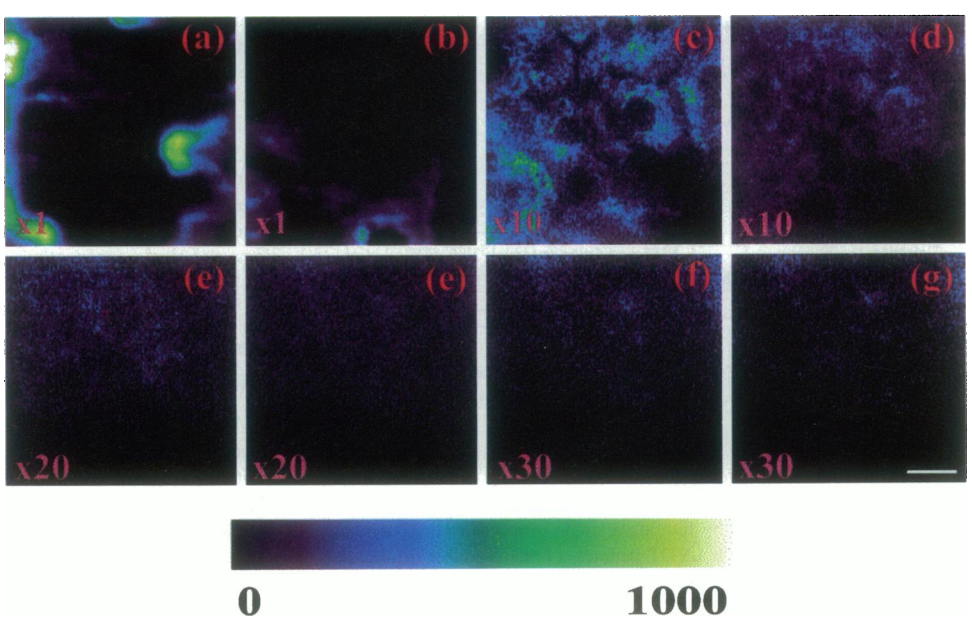

FIGURE 4 A montage of two-dimensional sections of in vivo human skin at successive depths. The excitation wavelength is 730 nm. The depth separation of each image is 20 μm. The scale bar corresponds to 10 μm.

were observed at depths from 40 μm to 80 μm, as seen in Fig. 4, *c–e*. These results are consistent with the cellular structures observed in the stratum spinosum by confocal microscopy and histological studies. Intensity variation is observed below 80 μm, but no structures can be discerned.

Two representative three-dimensional reconstructions of in vivo human skin obtained with two-photon excitation are presented. Fig. 5 *a* shows a 3-D reconstruction of 730-nm two-photon excitation images. This image is the same stack as the one used to generate the montage in Fig. 4. Three-dimensional reconstruction shows a bright fluorescent region that corresponds to the stratum corneum at the surface of the skin. A weaker fluorescent region extends from the bottom of the stratum corneum to the papillary dermis. The undulations of the papillary dermis are clearly seen in the *x-z* and *y-z* planes of the three-dimensional reconstruction. Although individual cells can be resolved in the *x-y* sections, they are not visible in the 3-D image because of their much lower intensity compared to that of the stratum corneum and the papillary dermis. Fig. 5 *b* shows a 3-D reconstruction of a 960 nm excited two-photon image stack. A much wider band of fluorescence is observed at the skin surface. This bright fluorescent region corresponds to the stratum corneum and most of the stratum spinosum. No individual cell layers have been discerned at this wavelength. Clearly, chromophores excited at 960 nm are different from those excited at 730 nm. These chromophores appear to distribute uniformly throughout the tissue and do not provide much contrast for discerning cellular structures.

Emission spectroscopy at selected points on the skin

At selected points on the skin, fluorescent spectra were measured close to the stratum corneum (0–50 μm) and deep inside the dermis (100–150 μm). Experiments were performed for both 730 nm (Fig. 6) and 960 nm (Fig. 7) excitation wavelengths corresponding to one-photon excitation wavelengths of about 365 nm and 480 nm, respectively.

Fig. 6 (*a* and *b*) shows typical fluorescent spectra obtained at different points in the 0–50-μm skin layer excited with 730 nm excitation. A bimodal peak is observed with maxima at 440 and 480 nm. The whole emission band is

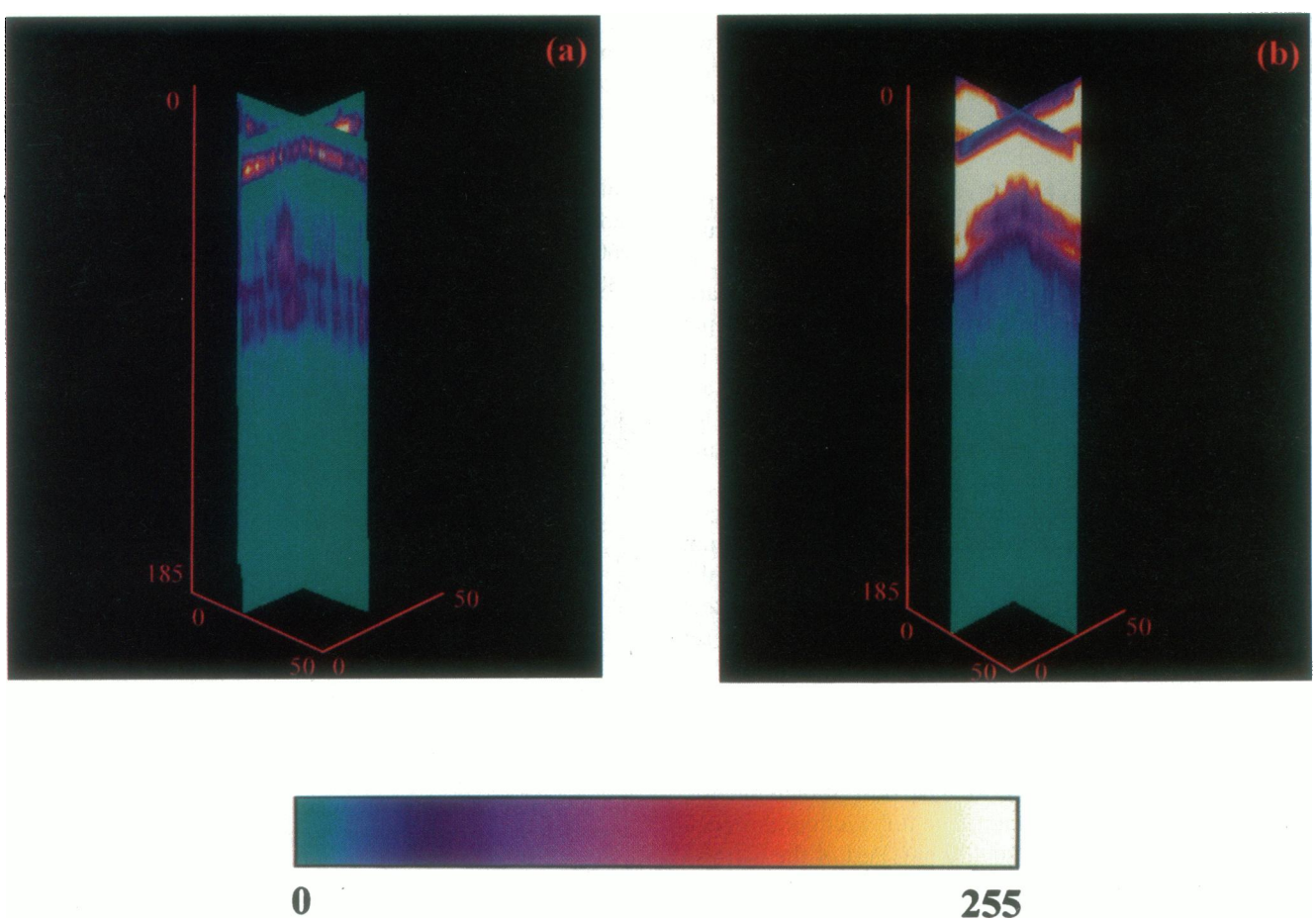

FIGURE 5 Three-dimensional images of in vivo human skin. (*a*) 730 nm excitation; (*b*) 960 nm excitation. *x* and *y* orthogonal slices are shown. The axis dimensions are in microns. In *a*, the top bright layer corresponds to the stratum corneum surface. The second bright band at a depth of 80–100 μm is the basal cell layer at the top of the papillary dermis. In *b*, the top bright band extends throughout the stratum corneum.

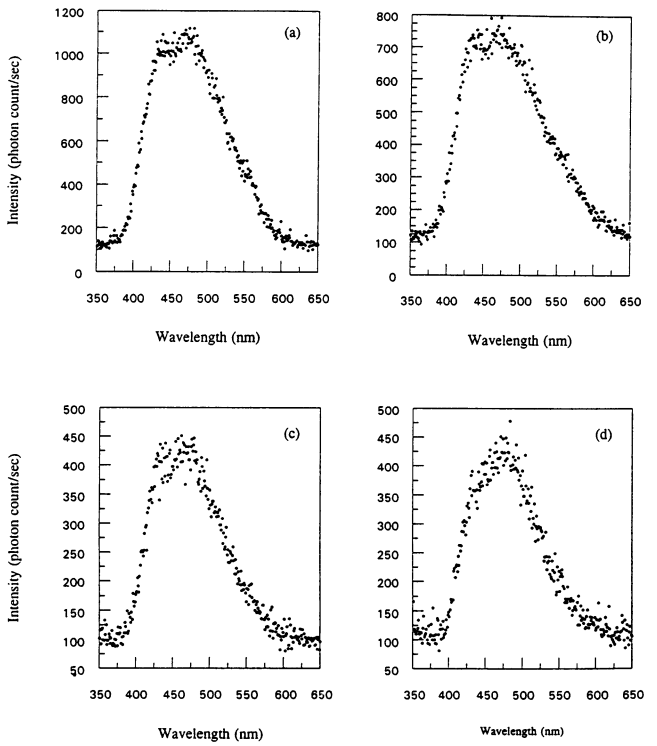

FIGURE 6 Point emission spectrum of in vivo human skin at 730-nm excitation. Intensity is given in photon counts per second. *a* and *b* are two distinct points on the surface of in vivo human skin between 0 and 50 μm deep. *c* and *d* are two distinct points at a depth between 100 and 150 μm.

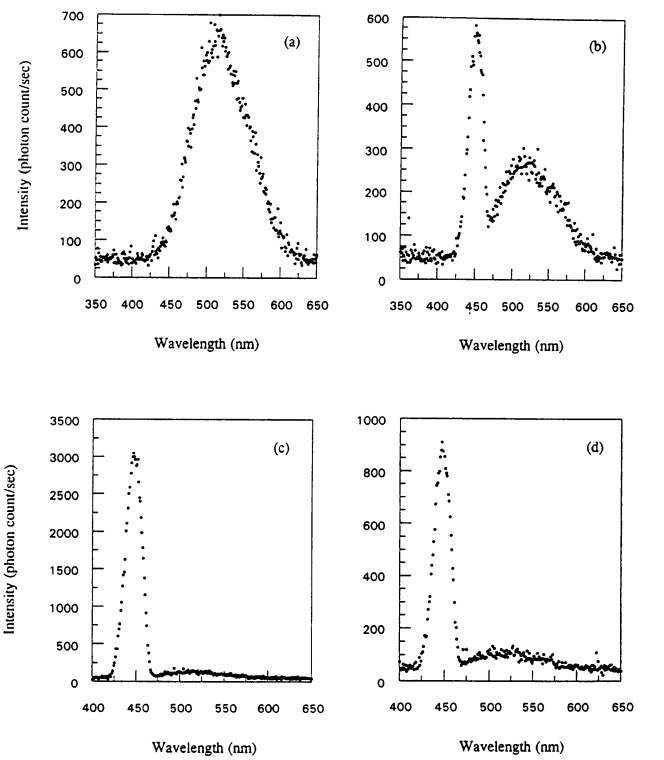

FIGURE 7 The point emission spectrum of in vivo human skin at 960-nm excitation. Intensity is given in photon counts per second. *a* and *b* are two distinct points on the surface of human skin between 0 and 50 μm deep. *c* and *d* are two distinct points at a depth between 100 and 150 μm.

wide, covering a region from 400 nm to 600 nm. At deeper regions (100–150 μm) (Fig. 6, *c* and *d*), the same spectrum is observed with some decrease in fluorescence intensity, as expected from the multiple scattering medium. The invariance of the fluorescence spectrum as a function of depth indicates that the same chemical species are present both on the surface and deep in the skin. The spectra observed are consistent with the emission of NAD(P)H cited in the literature, with an emission peak at 445–460 nm for 366-nm excitation (Chance and Thorell, 1959).

Fig. 7 (*a* and *b*) shows representative fluorescent spectra obtained in the 0–50-μm skin layer excited with 960-nm excitation. In contrast to the excitation at 730 nm, the spectrum observed is very position sensitive, indicating that at this wavelength we are exciting a very heterogeneous set of chromophores, and their distribution on the skin surface is uneven. At all skin positions measured, we have observed a broad emission peak centered at 520 nm, with a half-maximum spanning a range from 450 nm to 570 nm. At a few points on the skin surface we have observed an intense, narrow peak centered at 440 nm. The full width of this peak spans a range from 420 nm to 470 nm. Part of the narrowness of this peak observed may be due to the cut-on band-pass filter used, which starts attenuating wavelengths below 400 nm. However, the symmetry of this peak indicates that it is likely to be quite narrow. It is important to note that this emission peak cannot be caused by the two-photon process, but must have originated from a process involving three or more photons. All two-photon fluorescence caused by 960-nm excitation must emit at a wavelength longer than 480 nm. The observation of fluorescence emission at shorter

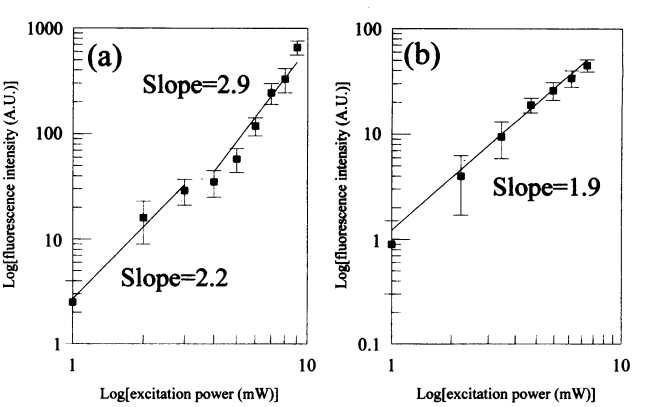

FIGURE 8 The fluorescence emission intensity as a function of laser excitation power at 960 nm. (*a*) At localized bright structures, the dependence of the fluorescence signal upon excitation intensity shows superquadratic dependence. At excitation intensity below 3 mW, fluorescence signal varies with excitation intensity with a power of 2.2, indicating a predominately two-photon process. At excitation power above 3 mW, fluorescence signal varies with excitation intensity with a power of 2.9, indicating a predominately three-photon process. (*b*) At lower intensity regions, the emission intensity shows quadratic dependence on the excitation intensity, indicating the presence of a two-photon process.

TABLE 1 Fluorescence emission spectra measured in in vivo human skin

Excitation (nm)	Depth (μm)	Component [1] center (nm)	Component [1] FWHM (nm)	Component [2] center (nm)	Component [2] FWHM (nm)
730	0–50	440	75	480	75
730	100–150	440	75	480	75
960	0–50	420	30	520	100
960	100–150	420	30	520	100

wavelengths indicates that the fluorescence originated from multiphoton processes. To verify this concept, fluorescence images as a function of excitation intensity at 960 nm were measured on a thin slice of freshly excised skin. These images show a low-intensity fluorescent background with localized high-intensity structures. The background region shows quadratic excitation power dependence, indicating that the fluorescence observed arose from the two-photon absorption process (Fig. 8 *b*). For some brighter structures, the fluorescence intensity shows superquadratic dependence on excitation intensity (Fig. 8 *a*). In particular, for excitation intensity below 3 mW, the fluorescence intensity is observed to vary with excitation at a power of 2.2, indicating a predominately two-photon process. However, this dependence switches to a power of 2.9 for excitation intensity above 3 mW, indicating the onset of a predominately three-photon process.

The spectra observed 100–150 μm deep into the dermis are presented in Fig. 7 (*c* and *d*). At this depth, the fluorescence spectrum is again rather invariant with position. The spectra in the deep tissue still show a broad peak background centered at 520 nm, but its intensity is much diminished. The spectra are dominated by the 440-nm peak, which is detected at all positions, and its intensity is significantly increased compared to the surface measurement. This observation indicates that the chromophore responsible for the 440-nm peak is much more abundant in deep tissue. The fluorescent emission component observed at 520 nm is consistent with the reported emission spectra of flavoproteins having a maximum from 520 to 550 nm for 366- or 460-nm excitation. The component contributing to the 420-nm emission remains to be identified in future studies.

In summary (Table 1), the fluorescence emission spectroscopy results are consistent with the following:

1. Two-photon excitation at 730 nm shows an emission spectrum consistent with NAD(P)H fluorescence at both the surface of the skin and at deeper levels up to 150 μm below the skin surface.

2. Multiphoton excitation at 960 nm shows an emission spectrum consistent with two-photon excited flavoprotein fluorescence peaking at 520 nm. The origin of a narrow emission component centered at 450 nm is of unknown origin and requires further characterization.

Fluorescence lifetimes at selected points on the skin

We have measured the fluorescence lifetime at selected points on the skin to complement the fluorescence spectral data obtained. The fluorescence lifetime is determined using frequency domain spectroscopy techniques (So et al., 1995). The fluorescence lifetime is determined at a modulation frequency of 80 MHz and is calculated from both the phase (τ_{phase}) and modulation (τ_{mod}) values. The lifetime results are summarized in Table 2. The large difference between the phase and modulation lifetimes indicates that there are multiple lifetime species contributing to the fluorescence signal. The coexistence of multiple fluorescent species is expected from the tissue heterogeneity. The literature values of NAD(P)H and flavoprotein reported ranges from 0.5 ns to 4 ns. The mean fluorescence lifetime for both excitation wavelengths is between 0.5 ns and 3 ns, which is consistent with NAD(P)H contributing at 730 nm excitation. The fluorescence lifetime measured at 960 nm is consistent with flavoprotein contribution. However, the existence of the additional component at 420 nm complicates interpretation at 960 nm and will require further work.

CONCLUSION

We have demonstrated the use of multiphoton excitation microscopy at 730 nm and 960 nm to image the autofluorescence of in vivo human skin from the surface to a depth of about 200 μm. The recording of emission spectra and fluorescent lifetime images further enables some characterization of the source of the autofluorescence. Our results support NAD(P)H as the primary source of the autofluorescence at 730 nm excitation. The chromophore composition responsible for 960 nm excitation is more complicated. Flavoproteins provide some contribution to the fluorescence signal. However, in deep tissue, the major fluorescence contribution originates from an unknown chromophore excited through multiphoton excitation. Multiphoton excitation opens the possibility of an optical biopsy of in vivo human skin based on functional imaging of cellular metabolites and therefore may have diagnostic potential in dermatology and the cell biology of in vivo human skin.

TABLE 2 Fluorescence lifetimes measured in in vivo human skin at 80 MHz

Excitation (nm)	Depth (μm)	τ_{phase} (ns)	τ_{mod} (ns)
730	0–50	0.5 ± 0.4	1.7 ± 0.7
730	100–150	1.0 ± 0.6	2.1 ± 0.7
960	0–50	0.23 ± 0.2	3.1 ± 2.0
960	100–150	0.55 ± 0.3	2.7 ± 2.0

This work was supported by a grant from NIH EY-06958 (BRM). The Laboratory for Fluorescence Dynamics, Department of Physics, is supported by the National Institutes of Health (RR03155).

REFERENCES

Bertrand, C., and P. Corcuff. 1994. In vivo spatio-temporal visualization of the human skin by real-time confocal microscopy. *Scanning.* 16: 150–154.

Chance, B. 1976. Pyridine nucleotide as an indicator of the oxygen requirements for energy-linked functions of mitochondria. *Circ. Res.* 38(Suppl. 1): I-31–I-38.

Chance, B., and M. Lieberman. 1978. Intrinsic fluorescence emission from the cornea at low temperature: evidence of mitochondrial signals and their differing redox states in epithelial and endothelial sides. *Exp. Eye Res.* 26:111–117.

Chance, B., and B. Schoener. 1966. Fluorometric studies of flavin component of the respiratory chain. *In* Flavins and Flavoproteins. E. C. Slater, editor. Elsevier Publishing Company, Amsterdam. 510–528.

Chance, B., B. Schoener, R. Oshino, F. Itshak, and Y. Nakase. 1979. Oxidation-reduction ratio studies of mitochondria in freeze-trapped samples. *J. Biol. Chem.* 254:4764–4711.

Chance, B., and B. Thorell. 1959. Localization and kinetics of reduced pyridine nucleotide in living cells by microfluorometry. *J. Biol. Chem.* 234:3044–3050.

Corcuff, P., C. Bertrand, and J. L. Leveque. 1993. Morphometry of human epidermis in vivo by real-time confocal microscopy. *Arch. Dermatol. Res.* 285:475–481.

Corcuff, P., and J. L. Leveque. 1993. In vivo vision of human skin with the tandem scanning microscope. *Dermatology.* 186:50–54.

Denk, W. J., J. H. Strickler, and W. W. Webb. 1990. Two-photon laser scanning fluorescence microscopy. *Science.* 248:73–76.

Dong, C. Y., P. T. C. So, T. French, and E. Gratton. 1995. Fluorescence lifetime imaging by asynchronous pump-probe microscopy. *Biophys. J.* 69:2234–2242.

Eng, J., R. M. Lynch, and R. S. Balaban. 1989. Nicotinamide adenine dinucleotide fluorescence spectroscopy and imaging of isolated cardiac myocytes. *Biophys. J.* 55:621–630.

Gryczynski, I., H. Malak, and J. R. Lakowicz. 1995a. Three-photon induced fluorescence of 2,5-diphenyloxazole with a femtosecond Ti-sapphire laser. *Chem. Phys. Lett.* 245:30–35.

Gryczynski, I., H. Malak, and J. R. Lakowicz. 1996. Three-photon excitation of a tryptophan derivative using a fs-Ti-sapphire laser. *Biospectroscopy.* 2:9–15.

Gryczynski, I., H. Szmacinski, and J. R. Lakowicz. 1995b. On the possibility of calcium imaging using indo-1 with three-photon. *Photochem. Photobiol.* 62:804–808.

Gu, M. 1996. Resolution in three-photon fluorescence scanning microscopy. *Optics Lett.* 21:988–990.

Koenig, K., P. T. C. So, W. W. Mantulin, B. J. Tromberg, and E. Gratton. 1996. Two-photon excited lifetime imaging of autofluorescence in cells during UVA and NIR photostress. *J. Microsc.* 183:197–204.

Masters, B. R. 1990. In vivo corneal redox fluorometry. *In* Noninvasive Diagnostic Techniques in Ophthalmology. B. R. Masters, editor. Springer-Verlag, New York. 223–247.

Masters, B. R. 1995. Confocal microscopy: history, principles, instruments, and some applicatins to the living eye. *Comm. Mol. Cell. Biophys.* 8:243–271.

Masters, B. R. 1996. Three-dimensional confocal microscopy of human skin in vivo: autofluorescence of normal skin. *Bioimages.* 4:13–19.

Masters, B. R., and B. Chance. 1993. Redox confocal imaging: intrinsic fluorescent probes of cellular metabolism. *In* Fluorescent and Luminescent Probes for Biological Activity. W. T. Mason, editor. Academic Press, London. 44–57.

Masters, B. R., G. Gonnord, and P. Corcuff. 1996. Three-dimensional microscopic biopsy of in vivo human skin: a new technique based on a flexible confocal microscope. *J. Microsc.* (in press).

Pawley, J. B., editor. 1995. Handbook of Biological Confocal Microscopy. Plenum Press, New York.

Petran, M., M. Hadravsky, M. D. Egger, and R. Galambos. 1958. Tandem scanning reflected light microscope. *J. Opt. Soc. Am.* 58:661–664.

Pierard, G. E. 1993. In vivo confocal microscopy: a new paradigm in dermatology. *Dermatology.* 186:4–5.

Piston, D. W., B. R. Masters, and W. W. Webb. 1995. Three-dimensionally resolved NAD(P)H cellular metabolic redox imaging of the in situ cornea with two-photon excitation laser scanning microscopy. *J. Microsc.* 178:20–27.

Rajadhyaksha, M., M. Grossman, D. Esterowitz, R. H. Webb, and R. R. Anderson. 1995. In vivo confocal scanning laser microscopy of human skin: melanin provides strong contrast. *J. Invest. Dermatol.* 104: 946–952.

Schneckenburger, H., and K. König. 1992. Fluorescence decay kinetics and imaging of NAD(P)H and flavins as metabolic indicators. *Opt. Eng.* 31:1447–1451.

So, P. T. C., T. French, W. M. Yu, K. M. Berland, C. Y. Dong, and E. Gratton. 1995. Time-resolved fluorescence microscopy using two-photon excitation. *Bioimaging.* 3:49–63.

So, P. T. C., T. French, W. M. Yu, K. M. Berland, C. Y. Dong, and E. Gratton. 1996. Two-photon fluorescence microscopy: time-resolved and intensity imaging. *In* Fluorescence Imaging and Microscopy. X. F. Wang and B. Herman, editors. Chemical Analysis Series, Vol. 137. John Wiley and Sons, New York. 351–374.

Szmacinski, H., I. Gryczynski, and J. R. Lakowicz. 1996. Three-photon induced fluorescence of the calcium probe indo-1. *Biophys. J.* 70: 547–555.

Wilson, T., editor. 1990. Confocal Microscopy. Academic Press, London.

Wokosin, D. L., V. E. Centonze, S. Crittenden, and J. G. White. 1995. *Mol. Biol. Cell.* 6:113a.

Xu, C., W. Zipfel, J. B. Shear, R. M. Williams, and W. W. Webb. 1996a. Multiphoton fluorescence excitation: new spectral windows for biological nonlinear microscopy. *Proc. Natl. Acad. Sci. USA.* 93:10763–10768.

Xu, C., W. Zipfel, and W. W. Webb. 1996b. Three photon excited fluorescence and application in nonlinear laser scanning microscopy. *Biophys. J.* 70:A429.